2000

Use of the generalized integral transform method for solving equations of solute transport in porous media

Chongxuan Liu
Pacific Northwest National Laboratory

Jim E. Szecsody
Pacific Northwest National Laboratory

John M. Zachara
Pacific Northwest National Laboratory, john.zachara@pnl.gov

William P. Ball
Johns Hopkins University

ELSEVIER

Advances in Water Resources 23 (2000) 483–492

Advances in Water Resources

Use of the generalized integral transform method for solving equations of solute transport in porous media

Chongxuan Liu [a,*], Jim E. Szecsody [a], John M. Zachara [a], William P. Ball [b]

[a] *Pacific Northwest National Laboratory, Richland, Washington 99352, USA*

[b] *Department of Geography and Environmental Engineering, Johns Hopkins University, Baltimore, MD 21218, USA*

Received 23 May 1999; accepted 14 October 1999

Abstract

The generalized integral transform technique (GITT) is applied to solve the one-dimensional advection–dispersion equation (ADE) in heterogeneous porous media coupled with either linear or nonlinear sorption and decay. When both sorption and decay are linear, analytical solutions are obtained using the GITT for one-dimensional ADEs with spatially and temporally variable flow and dispersion coefficient and arbitrary initial and boundary conditions. When either sorption or decay is nonlinear the solutions to ADEs with the GITT are hybrid analytical–numerical. In both linear and nonlinear cases, the forward and inverse integral transforms for the problems described in the paper are apparent and straightforward. Some illustrative examples with linear sorption and decay are presented to demonstrate the application and check the accuracy of the derived analytical solutions. The derived hybrid analytical–numerical solutions are checked against a numerical approach and demonstratively applied to a nonlinear transport example, which simulates a simplified system of iron oxide bioreduction with nonlinear sorption and nonlinear reaction kinetics.

1. Introduction

The mathematical simulation of solute transport in porous media commonly includes a need to model advection, dispersion, sorption, and reactions. Analytical, semi-analytical, and numerical approaches are frequently used in subsurface hydrology to solve these mathematical problems. Many analytical and semi-analytical solutions have been developed to simulate solute transport in porous media (e.g., [2,24]) and to check the accuracy of numerical approaches. However, past applications of the analytical and semi-analytical solutions have usually been limited to porous media with very simple and specific conditions that are pre-requisites to the finding of the solutions. Examples of such assumed conditions include homogeneous or specifically defined porous media (such as layered media), steady-state flow, and constant dispersion coefficient. In reality, subsurface porous media are seldom homogeneous and the properties of porous media are spatially and temporally variable [6,10]. The solute transport problems with these more complicated transport properties are not amenable to many of the traditional analytical approaches typically used in deriving analytical or semi-analytical solutions in subsurface hydrology, such as Laplace or Fourier transforms, for which difficulties can be associated with both forward and inverse transforms. Therefore, numerical approaches have been more widely applied to simulate these complicated cases. To date, analytical or semi-analytical solutions to test and validate the numerical approaches under many complex conditions have not been available.

The objective of this paper is to present solutions for one-dimensional solute transport problems coupled with either linear or nonlinear sorption and/or decay and with conditions that allow temporally and/or spatially variable flow $(v(x,t))$ and dispersion coefficient $(D(x,t))$, as well as space-variable initial and time-variable boundary conditions. The generalized integral transform technique (GITT) [5,16] is used in this paper due to its flexibility in facilitating the construction of an integral transform pair (forward and inverse transforms) and the relative ease with which the resulting integral transform pair can be mathematically manipulated. The GITT has been developed and described with regard to its use in the derivation of unified analytical solutions for linear heat transfer and mass diffusion problems [16],

* Corresponding author.

0309-1708/00/$ - see front matter
PII: S0309-1708(99)00048-2

and the method has recently been advanced to include nonlinear problems of heat transfer and fluid flow [5]. However, the application of the GITT to solve solute transport problems in subsurface hydrology has not been widely explored. A few cases include Almeida and Cotta [1], who demonstrated how this method could be used to derive an analytical solution to a two-dimensional linear transport problem in homogeneous porous media; and Liu and others [14], who applied this technique to derive an analytical solution for one-dimensional solute transport in heterogeneous porous media (approximated by multi-layer). The approach used and problems solved in this paper significantly extends the prior work of Liu et al. [14]. First, the assumed values of flow velocity and dispersion coefficient are allowed to be arbitrary functions of space and time. The solutions derived with this extension thus allow the handling of more complicated problems, such as those where the properties of porous media change spatially and temporally. Second, in the work presented here, we include a possibility for sorption and decay which can be either linear or nonlinear in its mathematical formulation. More specifically, the present paper describes how the GITT can be used to derive analytical solutions for solute transport problems in porous media with spatially and temporally variable flow and dispersion coefficient coupled with linear sorption and decay, and to derive hybrid analytical-numerical solutions when sorption and/or decay is nonlinear.

2. Problem formulation and solution

We begin by considering the following general one-dimensional mathematical model of solute transport in porous media:

$$R(C,x)\frac{\partial C}{\partial t} = \frac{\partial}{\partial x}\left(D(x,t)\frac{\partial C}{\partial x}\right) - v(x,t)\frac{\partial C}{\partial x} + I(C,x,t), \tag{1a}$$

which describes processes of advection, dispersion, equilibrium sorption, and decay. In Eq. (1a), C denotes the aqueous solute concentration; $D(x,\ t)$ is dispersion coefficient; $v(x,t)$ is linear velocity; $R(C,\ x)$ is retardation factor; and $I(C,\ x,\ t)$ is rate of decay per unit volume of aqueous solution. Both $D(x,\ t)$ and $v(x,\ t)$ are assumed generally to be functions of space (x) and time (t); $R(C,\ x)$ is assumed to be a function of concentration (C) and space (x); and the decay rate is assumed to be a function of concentration (C), space (x), and time (t). All terms will be a function of the physical and geometric properties of the porous medium (e.g., porosity and bulk density). Eq. (1a) is subjected to following general boundary and initial conditions [7,20,24,25]:

$$v(x,t)C(x,t) - D(x,t)\frac{\partial C(x,t)}{\partial x}\bigg|_{x=0} = v(x=0,t)f(t), \tag{1b}$$

$$\frac{\partial C(x,t)}{\partial x}\bigg|_{x=L} = 0, \tag{1c}$$

$$C(x,t)|_{t=0} = F(x), \tag{1d}$$

where L is the length of the porous medium.

The solution method begins with variable substitution in Eq. (1a) in order to make the inlet boundary condition (1b) homogeneous, thus improving overall convergence behavior of the solution at the inlet boundary point [1,5,14]

$$C(x,t) = U(x,t) + f(t), \tag{2}$$

where $U(x,t)$ is the solution of following problem:

$$R(C,x)\frac{\partial U}{\partial t} = \frac{\partial}{\partial x}\left(D(x,t)\frac{\partial U}{\partial x}\right) - v(x,t)\frac{\partial U}{\partial x} - R(C,x)\frac{\mathrm{d}f(t)}{\mathrm{d}t} + I(C,x,t) \tag{3}$$

with $R(C,x), D(x), v(x), I(C,x,t)$ defined as before.

$U(x,t)$ has the same forms of boundary conditions as (1b) and (1c) but with the right side now set equal to zero for both equations.

The initial condition of $U(x,t)$ becomes

$$U(x,t)|_{t=0} = F(x) - f(0).$$

In order to solve problem (3) through the GITT, a pair of transforms, namely an integral transform and an inverse transform, has to be established [1,5,14]. For the current problem (3), we select the following auxiliary problem, because of its simplicity for the purpose of constructing the pair of transforms:

$$\frac{\mathrm{d}^2\varphi_n(x)}{\mathrm{d}x^2} + \beta_n^2\varphi_n(x) = 0 \quad n = 1,2,\ldots,\infty \tag{4a}$$

with the following boundary conditions:

$$v_0\varphi_n(x) - D_0\frac{\mathrm{d}\varphi_n(x)}{\mathrm{d}x}\bigg|_{x=0} = 0, \tag{4b}$$

$$\frac{\mathrm{d}\varphi_n(x)}{\mathrm{d}x}\bigg|_{x=L} = 0, \tag{4c}$$

where β_n and $\varphi_n(x)$ are nth eigen value and its corresponding eigen function, respectively. The values of constant v_0 and D_0 are $v(x,t)$ and $D(x,t)$ at $x=0, t=0$.

Auxiliary problem (4) has the following eigen function and norm [19]:

$$\varphi_n(x) = \cos(\beta_n(L-x)), \quad N_n = \frac{1}{2}\left(L + \frac{v_0 D_0}{\beta_n^2 D_0^2 + v_0^2}\right)$$

respectively, and its eigen value is determined from the following equation:

$$v_0\cos(\beta_n L) - D_0\beta_n\sin(\beta_n L) = 0.$$

Having obtained the eigen functions for the system (4), we can construct [5,16], the forward transform

$$T_n(t) = \frac{1}{N_n^{1/2}} \int_0^L \varphi_n(x) U(x,t)\,\mathrm{d}x \tag{5}$$

and its corresponding inverse transform

$$U(x,t) = \sum_{n=1}^{\infty} \frac{1}{N_n^{1/2}} \varphi_n(x) T_n(t). \tag{6a}$$

From a computational point of view, inverse transform (6a) is truncated at its Mth term with M selected at a value large enough to produce the desired level of accuracy. Thus, we write inverse transform (6a) as

$$U(x,t) = \sum_{n=1}^{M} \frac{1}{N_n^{1/2}} \varphi_n(x) T_n(t). \tag{6b}$$

Eq. (6b) involves $T_n(t)$ terms $(n = 1,2,\ldots,M)$, which have to be determined from Eq. (3). In order to derive $T_n(t)$, we apply the operator $\int_0^L (\varphi_n(x))/(N_n^{1/2})\,\mathrm{d}x$ to Eq. (3) to obtain

$$\begin{aligned}
&\frac{1}{N_n^{1/2}} \int_0^L \varphi_n(x) R(C,x) \frac{\partial U}{\partial t}\,\mathrm{d}x \\
&\quad = \frac{1}{N_n^{1/2}} \int_0^L \varphi_n(x) \frac{\partial}{\partial x}\left(D(x,t) \frac{\partial U}{\partial x} \right) \mathrm{d}x \\
&\quad - \frac{1}{N_n^{1/2}} \int_0^L \varphi_n(x) v(x,t) \frac{\partial U}{\partial x}\,\mathrm{d}x \\
&\quad - \frac{1}{N_n^{1/2}} \int_{x0}^L R(C,x) \varphi_n(x) \frac{\mathrm{d}f(t)}{\mathrm{d}t}\,\mathrm{d}x \\
&\quad + \frac{1}{N_n^{1/2}} \int_{x0}^L I(C,x,t) \varphi_n(x)\mathrm{d}x.
\end{aligned} \tag{7}$$

After rearrangement and using inverse transform (6b), Eq. (7) becomes:

$$\begin{aligned}
&\sum_{r=1}^{M} A_{nr}(\mathbf{T}) \frac{\mathrm{d}T_r(t)}{\mathrm{d}t} + \sum_{r=1}^{M} B_{nr}(t) T_r(t) = g_n(T,t) \\
&n = 1,2,\ldots,M,
\end{aligned} \tag{8}$$

where

$$A_{nr}(\mathbf{T}) = \int_0^L \frac{\varphi_n(x)\varphi_r(x)}{N_n^{1/2} N_r^{1/2}} R(C,x)\,\mathrm{d}x,$$

$$\begin{aligned}
B_{nr}(t) = \frac{1}{N_n^{1/2} N_r^{1/2}} \int_0^L \Bigg(& v(x,t)\varphi_n(x) \frac{\mathrm{d}\varphi_r(x)}{\mathrm{d}x} \\
& - \varphi_r(x) \frac{\mathrm{d}}{\mathrm{d}x}\left(D(x,t) \frac{\mathrm{d}\varphi_n(x)}{\mathrm{d}x} \right) \Bigg) \mathrm{d}x \\
& + \frac{1}{N_n^{1/2} N_r^{1/2}} \Bigg(v(x=0,t)\varphi_n(0)\varphi_r(0) \\
& - D(x=0,t)\varphi_r(0) \frac{\mathrm{d}\varphi_n(0)}{\mathrm{d}x} \Bigg),
\end{aligned}$$

$$g_n(\mathbf{T},t) = \int_0^L \frac{\varphi_n(x)}{N_n^{1/2}} \left(I(C,x,t) - R(C,x) \frac{\mathrm{d}f(t)}{\mathrm{d}t} \right) \mathrm{d}x.$$

In matrix form, system (8) becomes

$$A(\mathbf{T}) \frac{\mathrm{d}\mathbf{T}(t)}{\mathrm{d}t} + \mathbf{B}(t)\mathbf{T}(t) = \mathbf{G}(\mathbf{T},t). \tag{9a}$$

Here matrix $\mathbf{A}(\mathbf{T})$ is a symmetric positive definite matrix (see Appendix A). This property is exploited in subsequent development, such as finding the inverse to the matrix, and in numerically solving Eq. (9a).

The initial condition for Eq. 9(a) can be derived by applying integral transform (5) to initial condition of problem (3)

$$T_n(0) = \int_0^L \frac{\varphi_n(x)}{N_n^{1/2}} (F(x) - f(0))\,\mathrm{d}x. \tag{9b}$$

Once one solves for the set of coupled first-order differential equations described by (9a) and (9b), inverse formula (6b) can be called to calculate $U(x,t)$, and Eq. (2) used to calculate concentration $C(x,t)$. Generally, problem (9) has to be solved numerically; however in linear cases these equations can be solved analytically. In the next section, we will derive and discuss these analytical solutions under various conditions. For nonlinear cases, problem (9) may be solved by applying, to a prescribed level of accuracy, any of several nonlinear ordinary differential equation solvers found in many public math libraries, such as the IMSL library [13]. In Section 4, we will give some illustrative examples to demonstrate how we can use GITT to solve nonlinear transport problems.

3. Analytical solutions

In this section, we demonstrate the use of the GITT to derive a general analytical solution to solute transport problem with spatially and temporally variable flow and dispersion coefficient when coupled with linear sorption and decay. The linearity of both sorption and decay are required in order to solve Eq. (9a) analytically. Because all mathematical procedures used in Eqs. (9a) and (9b) are analytical, the complete analytical solution to problem (1) only requires that we analytically solve a set of first order differential equations described by (9a) and (9b).

When both sorption and decay are linear $(R(C,x) = R(x); I(C,x,t) = \lambda_0(x,t) - \lambda_1(x,t)C)$, Eq. (9a) can be simplified as follows:

$$\mathbf{A} \frac{\mathrm{d}\mathbf{T}(t)}{\mathrm{d}t} + \mathbf{B}(t)\mathbf{T}(t) = \mathbf{G}(t), \tag{10}$$

where

$$A_{nr} = \int_0^L \frac{\varphi_n(x)\varphi_r(x)}{N_n^{1/2} N_r^{1/2}} R(x)\,\mathrm{d}x,$$

$$B_{nr}(t) = \frac{1}{N_n^{1/2}N_r^{1/2}}\int_0^L \left(v(x,t)\varphi_n(x)\frac{\mathrm{d}\varphi_r(x)}{\mathrm{d}x} - \varphi_r(x)\frac{\mathrm{d}}{\mathrm{d}x}\left(D(x,t)\frac{\mathrm{d}\varphi_n(x)}{\mathrm{d}x}\right)\right)\mathrm{d}x + \frac{1}{N_n^{1/2}N_r^{1/2}}\left(v(x=0,t)\varphi_n(0)\varphi_r(0) - D(x=0,t)\varphi_r(0)\frac{\mathrm{d}\varphi_n(0)}{\mathrm{d}x}\right) + \frac{1}{N_n^{1/2}N_r^{1/2}}\int_0^L \lambda_1(x,t)\varphi_n(x)\varphi_r(x)\,\mathrm{d}x$$

$$g_n(t) = \int_0^L \frac{\varphi_n(x)}{N_n^{1/2}}\left(\lambda_0(x,t) - R(x)\frac{\mathrm{d}f(t)}{\mathrm{d}t} - \lambda_1(x,t)f(t)\right)\mathrm{d}x.$$

Here concentration (C) in the term, $\lambda_1(x,t)C$, is replaced by its inverse transform (6b) and its nonlinear part has been moved from $g_n(t)$ to $B_{nr}(t)$ in order to make $g_n(t)$ linear. Eq. (10) forms a typical linear system that has a following form of analytical solution [22]:

$$\mathbf{T}(t) = \boldsymbol{\Phi}(t,0)\mathbf{T}(0) + \int_0^t \boldsymbol{\Phi}(t,\tau)\mathbf{A}^{-1}\mathbf{G}(\tau)\,\mathrm{d}\tau, \tag{11}$$

where $\boldsymbol{\Phi}(t,\tau)$ is a transition matrix, also called the *Peano–Baker Series* in linear system theory [22]. Transition matrix, $\boldsymbol{\Phi}(t,\tau)$, is defined as follows:

$$\boldsymbol{\Phi}(t,\tau) = \mathbf{I} + \int_\tau^t \mathbf{P}(\sigma_1)\mathrm{d}\sigma_1 + \int_\tau^t \mathbf{P}(\sigma_1)\int_\tau^{\sigma_1}\mathbf{P}(\sigma_2)\,\mathrm{d}\sigma_2\,\mathrm{d}\sigma_1 + \int_\tau^t \mathbf{P}(\sigma_1)\int_\tau^{\sigma_1}\mathbf{P}(\sigma_2)\int_\tau^{\sigma_2}\mathbf{P}(\sigma_3)\,\mathrm{d}\sigma_3\,\mathrm{d}\sigma_2\,\mathrm{d}\sigma_1 + \cdots, \tag{12}$$

where $\mathbf{P}(t) = -\mathbf{A}^{-1}\mathbf{B}(t)$.

Theoretically speaking, Eqs. (2), (6b) and (11), provide a general analytical solution for problem (1) with linear sorption and decay in porous media and with time- and space-variable parameters. To our knowledge, this analytical solution is new, or at least has not been previously published in peer-reviewed literature. The transition matrix, $\boldsymbol{\Phi}(t,\tau)$, which has been extensively discussed in linear system theory, should have desirable mathematical properties similar to an exponential function [22]. For practical purposes of simulating solute transport problems, the applicability of the analytical solution described by (2), (6b) and (11) will therefore strongly depend on the degree of difficulty in evaluating this transition matrix, $\boldsymbol{\Phi}(t,\tau)$. In the rest of this section, we will discuss two broad classes of problems for which the transition matrix can be significantly simplified so that the analytical solution described by Eqs. (2), (6b) and (11), can be of practical value.

3.1. Steady state flow, dispersion coefficient, and decay

For steady state flow, dispersion coefficient, and decay, $\mathbf{B}(t)$ matrix in Eq. (10) becomes constant. In these cases, transition matrix $\boldsymbol{\Phi}(t,\tau)$ can be simplified into a matrix exponential and solution (11) becomes,

$$\mathbf{T}(t) = \exp(-\mathbf{A}^{-1}\mathbf{B}t)\mathbf{T}(0) + \exp(-\mathbf{A}^{-1}\mathbf{B}t) \times \int_0^t \exp(\mathbf{A}^{-1}\mathbf{B}\tau)\mathbf{A}^{-1}\mathbf{G}(\tau)\,\mathrm{d}\tau, \tag{13}$$

where:

$$A_{nr} = \int_0^L \frac{\varphi_n(x)\varphi_r(x)}{N_n^{1/2}N_r^{1/2}}R(x)\,\mathrm{d}x,$$

$$B_{nr} = \frac{1}{N_n^{1/2}N_r^{1/2}}\int_0^L \left(v(x)\varphi_n(x)\frac{\mathrm{d}\varphi_r(x)}{\mathrm{d}x} + D(x)\frac{\mathrm{d}\varphi_r(x)}{\mathrm{d}x}\frac{\mathrm{d}\varphi_n(x)}{\mathrm{d}x}\right)\mathrm{d}x + \frac{1}{N_n^{1/2}N_r^{1/2}}v(0)\varphi_r(0)\varphi_n(0) + \frac{1}{N_n^{1/2}N_r^{1/2}}\int_0^L \lambda_1(x)\varphi_n(x)\varphi_r(x)\,\mathrm{d}x,$$

$$G_n(t) = G_{1n} + G_{2n}\frac{\mathrm{d}f(t)}{\mathrm{d}t} + G_{3n}f(t)$$

$$G_{1n} = \int_0^L \frac{\varphi_n(x)}{N_n^{1/2}}\lambda_0(x)\,\mathrm{d}x$$

$$G_{2n} = -\int_0^L \frac{\varphi_n(x)}{N_n^{1/2}}R(x)\,\mathrm{d}x,$$

$$G_{3n} = -\int_0^L \frac{\varphi_n(x)}{N_n^{1/2}}\lambda_1(x)\,\mathrm{d}x;$$

Eqs. (2), (6b) and (13), form an analytical solution for solute transport problems in heterogeneous porous media with space-variable parameters $(R(x), D(x), v(x), \lambda_0(x), \lambda_1(x))$. Compared with the analytical solution in heterogeneous porous media by Liu et al. [14], the current solution is more flexible in dealing with various porous media properties because the parameters, $R(x), D(x), v(x), \lambda_0(x), \lambda_1(x)$, can now be treated as arbitrary functions. The matrix exponential in Eq. (13) can be efficiently and accurately evaluated using an eigen value method which has been detailed elsewhere [17]. Constant matrices of $\mathbf{A}$ and $\mathbf{B}$, and vectors $\mathbf{G}_1$, $\mathbf{G}_2$, and $\mathbf{G}_3$ can be evaluated either analytically or numerically depending on the function properties in corresponding integrals. When a numerical method is used to evaluate these constant matrices or vectors, Fast Fourier Transform can be used to accurately and efficiently perform the integration [21].

Fig. 1 shows two simple examples that are used to verify our current solution against two analytical solutions previously developed for the simple case of

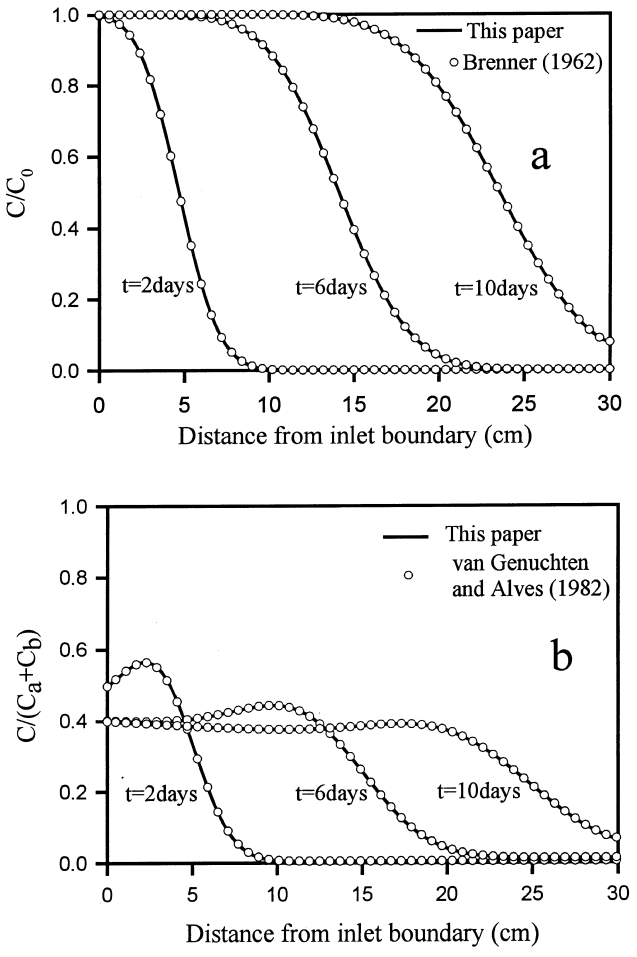

Fig. 1. Concentration changes in a homogeneous porous medium. Fig. 1(a) shows a case with zero initial concentration, constant inlet condition ($f(t) = C_0$), and no decay. Parameters used: medium length (L) = 30 cm, retardation factor (R) = 4.25, velocity (v) = 10 cm/d, dispersion coefficient (D) = 4 cm^2/d. Fig. 1(b) shows the same case as in Fig. 1(a) except that inlet concentration is a function of time ($f(t) = C_a + C_b \exp(-t), C_a = 0.4$ and $C_b = 0.6$) and there is a decay ($I(C) = -0.1C + 0.01$) l/d.

homogeneous porous medium (Fig. 1(a) for constant inlet condition and no decay and Fig. 1(b) for variable inlet condition and decay). As shown in these figures, the numerical values generated by the current analytical solution are identical to the results from Brenner's solution [3] for the case of constant inlet boundary condition and a solution by van Genuchten and Alves [24] for the time-variable inlet boundary condition. In the examples, the convergence of the series solution (6b) requires approximately 30 terms. Here the convergence of the series solution (6b) is assumed when the difference between the calculated concentrations using truncated series and "complete series" (here complete series is represented by the solution (6b) with 300 terms) is less than 0.1%. Both solutions provided by Brenner [3] and van Genuchten and Alves [24] also require roughly about 30 terms to converge.

Fig. 2(a) and (b) show an example in a heterogeneous porous medium with continuously space-varying functions of transport parameters. Fig. 2(a) shows concentration distribution (solid line) at $t = 2$ days. It also shows concentration distributions when the continuously space-variable parameters are simulated assuming one-layer-averaged (dash line) and two-layer-averaged (dotted line) approximation of the porous medium. For the two-layer case, the two layers are separated at the center of the medium. It is apparent that the concentration distribution from the one-layer-averaged model is different from the true model, while the two-layer-averaged model is able to closely simulate that reflected by the "true" model (Fig. 2(a)). With an increase in the number of layers considered, a layer-averaged model can better approximate a heterogeneous system. In this

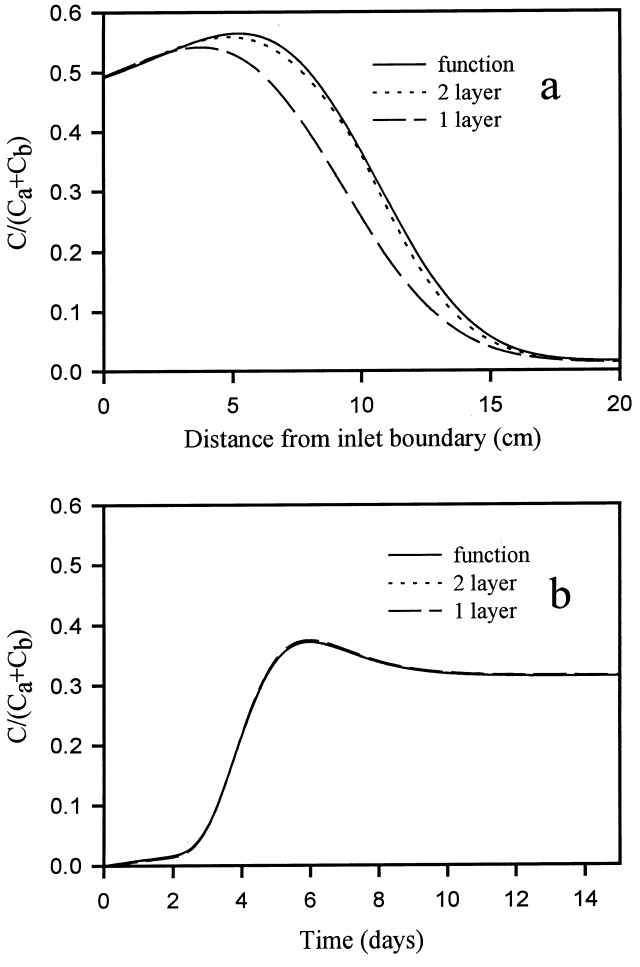

Fig. 2. Concentration changes in a heterogeneous porous medium. Fig. 2(a) shows concentration distributions in the porous medium (L = 20 cm) at time ($t = 2$ days) for three cases: (1) (solid line) the porous medium has properties, $R = 2.4 + 0.04x$, $v = 14 - 0.2x$ cm/d, $D = 10 - 0.1x$ cm^2/d, $I(C) = -(0.1 + 0.01x)C + 0.001x + 0.01$ l/d, ($f(t) = C_a + C_b \exp(-t), C_a = 0.4$ and $C_b = 0.6$); (2) one layer porous medium with average properties of case (1); (3) two layer porous medium with average properties of case (1). Fig. 2(b) shows breakthrough curves of three cases described in Fig. 2(a).

example, a five-layer-averaged model can very closely approximate the heterogeneous medium with continuously variable parameters over space (data not shown).

Fig. 2(b) shows that the breakthrough curves from the true and both of the two approximated models are very close to each other. This result indicates that breakthrough curves may not be a sensitive means of detecting heterogeneity of porous media. Although breakthrough curves can be used to estimate parameters for any of assumed physical model, we should not expect "goodness-of-fit" criteria to provide much indication of the accuracy of our assumed physical model, vis-à-vis actual variations (and locations of variation) for the physical properties of the porous medium.

3.2. Transitional flow and decay in homogeneous porous media

Another class of transport problems for which the evaluation of the transitional matrix $\boldsymbol{\Phi}(t,\tau)$ (12) can be significantly simplified is under an assumption that the porous medium is homogeneous and

$$D(t) = \alpha_L v(t), \tag{14}$$

where α_L is a longitudinal dispersivity. In this class of problems, the flow velocity, resulting dispersion coefficient, and decay rate are all allowed to change with time. Assumption (14) is often used to describe solute transport in porous media with dispersion dominated by mechanical properties of the porous medium [2,9]. Under these assumptions, the coefficients in matrix Eq. (9a) becomes,

$$A_{nr} = R\delta_{nr},$$

$$B_{nn}(t) = v(t)\left(\alpha_L\beta_n^2 + \frac{1-\cos^2(\beta_n L)}{2N_n}\right) + \lambda_1(t),$$

$$B_{nr}(t) = v(t)(\beta_r^2(1-\cos(\beta_n L)\cos(\beta_r L)) - \beta_n\beta_r\sin(\beta_n L)\sin(\beta_r L))/(N_n^{1/2}N_r^{1/2}(\beta_r^2-\beta_n^2)) \quad n\neq r,$$

$$g_n(t) = \left(\lambda_0(t) - R\frac{\mathrm{d}f(t)}{\mathrm{d}t} - \lambda_1(t)f(t)\right)\frac{\sin(\beta_n L)}{\beta_n N_n^{1/2}}.$$

With these coefficients, we obtain the following relationship:

$$\mathbf{P}(t)\int_\tau^t \mathbf{P}(\sigma)\,\mathrm{d}\sigma = \int_\tau^t \mathbf{P}(\sigma)\,\mathrm{d}\sigma\mathbf{P}(t), \tag{15}$$

$$\mathbf{P}(t) = -\mathbf{A}^{-1}\mathbf{B}(t) = -\frac{v(t)}{R}\mathbf{B}_1 - \frac{\lambda_1(t)}{R}\mathbf{I},$$

where $\mathbf{P}$ matrix is defined before and $\mathbf{I}$ is identity matrix and constant matrix $\mathbf{B}_1$ has following constant elements:

$$B1_{nn} = \left(\alpha_L\beta_n^2 + \frac{1-\cos^2(\beta_n L)}{2N_n}\right),$$

$$B1_{nr} = \frac{\beta_r^2(1-\cos(\beta_n L)\cos(\beta_r L)) - \beta_n\beta_r\sin(\beta_n L)\sin(\beta_r L)}{N_n^{1/2}N_r^{1/2}(\beta_r^2-\beta_n^2)} \quad n\neq r.$$

Using the relationship (15), the transition matrix, $\boldsymbol{\Phi}(t,\tau)$, can be simplified as follows [22]:

$$\boldsymbol{\Phi}(t,\tau) = \exp\left(\int_\tau^t \mathbf{P}(\sigma)\,\mathrm{d}\sigma\right) = \exp\left(-\frac{1}{R}\int_\tau^t \lambda_1(\sigma)\,\mathrm{d}\sigma\right)\exp\left(-\frac{1}{R}\mathbf{B}1\int_\tau^t v(\sigma)\,\mathrm{d}\sigma\right).$$

As described before, this matrix exponential can be accurately and efficiently evaluated using a previously described eigen value method [17]. Using (16), we have

$$\begin{aligned}\mathbf{T}(t) = {} & \exp\left(-\frac{1}{R}\int_0^t \lambda_1(\sigma)\,\mathrm{d}\sigma\right) \\ & \times \exp\left(-\frac{\mathbf{B}_1}{R}\int_0^t v(\sigma)\mathrm{d}\sigma\right)T(0) \\ & + \int_0^t \exp\left(-\frac{1}{R}\int_\tau^t \lambda_1(\sigma)\mathrm{d}\sigma\right) \\ & \times \exp\left(-\frac{\mathbf{B}_1}{R}\int_\tau^t v(\sigma)d\sigma\right)G(\tau)\,\mathrm{d}\tau.\end{aligned} \tag{17}$$

Note that for this class of problems, D_0 and v_0 in the boundary condition for (4b) can be taken as α_L and 1, respectively. Thus, the solution (6b) automatically satisfies the inlet boundary condition for (3), regardless of how velocity may change with time.

Fig. 3 shows an example of solute transport under conditions of time-increasing flow velocity and dispersion coefficient. As shown in Fig. 3, the concentration profiles are steeper at short time than at longer time, indicating that dispersion increases with time. This is an expected result, given that the dispersivity (0.1 cm) is held constant and that velocity is increasing with time.

4. Analytical–numerical solution

When either decay, sorption, or both are nonlinear, then the solution to problem (1) becomes a hybrid analytical–numerical solution. This is because solution (6b) is analytic only with respect to the spatial variable, and the temporal part needs to be solved numerically from problem (9). In the examples explored subsequently, problem (9) is solved through the use of an adaptive ordinary differential equation solver, DIVPAG, found in the IMSL library [13]. The coefficients in Eqs. (9a) and (9b) are updated using Fast Fourier Transform [13,21]. Generally speaking, solutions for nonlinear transport problems under the GITT converge

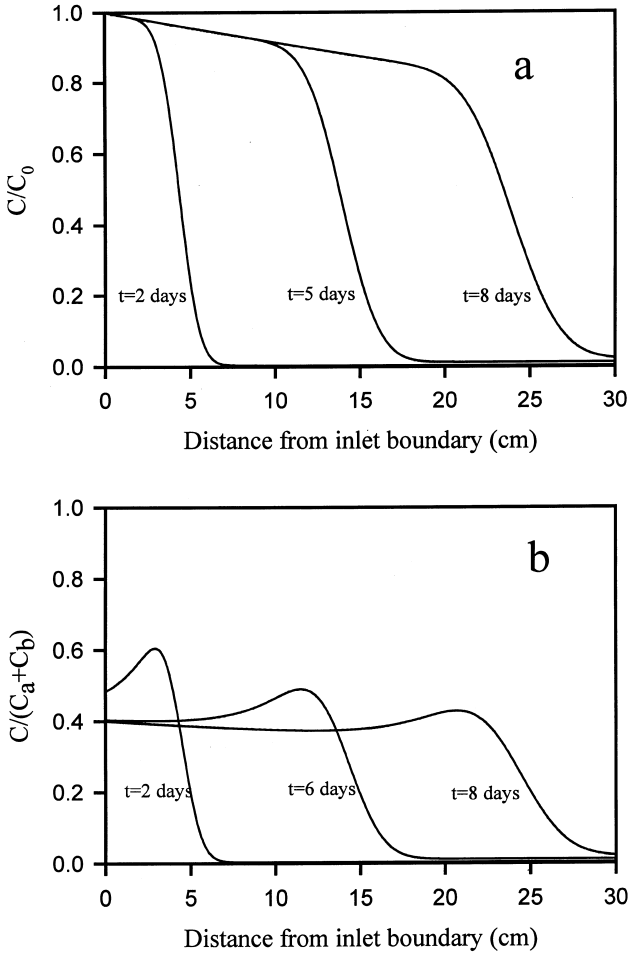

Fig. 3. Concentration changes in a homogeneous porous medium with time-variable parameters. Fig. 3(a) shows a case with $L = 30$ cm $D(t) = 0.1v(t)$ cm^2/d; $v(t) = 10 - 8\exp(-t)$ cm/d; $I(C) = -0.1(1-\exp(-t))C + 0.01(1 - \exp(-t))$ l/d; $R = 3$; $f(t) = C_0$; Fig. 3(b) shows the same case as in Fig. 4(a) except that $f(t) = C_a + C_b\exp(-t)$, $C_a = 0.4$ and $C_b = 0.6$.

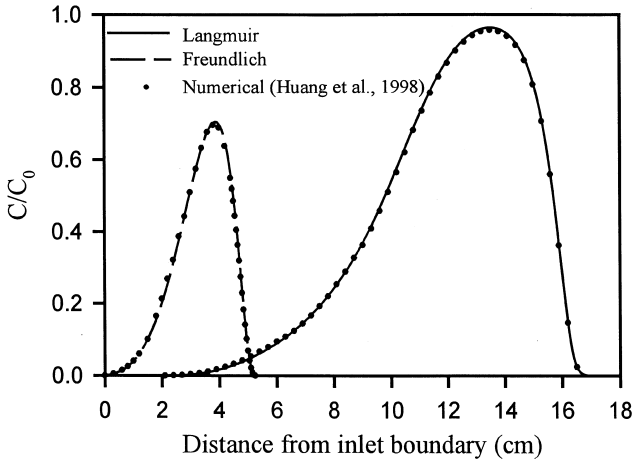

Fig. 4. Concentration distribution ($t = 190$ s) derived from hybrid analytical–numerical solution and Modified Picard Iteration numerical method for cases with nonlinear sorption. (dispersion coefficient, $D = 0.01$ cm^2/s; flow rate, $v = 0.1$ cm/s; bulk density, $\rho_b = 1.687$ g/cm^3; porosity, $\varepsilon = 0.37$; sorbed concentration, $S = 0.3C^{0.7}$ (Freundlich), $= 0.3C/(1 + 100C)$ mg/kg (Langmuir). (Example after Goode and Konikow [11], Huang et al. [12].)

slowly and intensive computational effort is required compared with pure numerical approaches. For the two examples that will be discussed subsequently, approximately 100 terms are required to reach convergence. Most of the computational cost of GITT for nonlinear problems lies in updating the coefficients in Eqs. (9a) and (9b). However, GITT can provide a highly accurate solution to nonlinear problems [5]. This is because a solution to the finite nonlinear system (9) will converge to a solution to the corresponding infinite system for sufficiently large M [4] and all of numerical procedures used in this approach can be controlled to achieve a prescribed level of accuracy. Thus the hybrid analytical–numerical solution may have a substantial value as a benchmark for numerical methods.

Fig. 4 shows an example for problems of solute transport with nonlinear sorption that has been explored by Goode and Konikow [11] and recently by Huang et al. [12] using pure numerical approaches. Due to its high accuracy of mass balance, the numerical approach (Modified Picard Iteration Method) described by Huang et al. [12] is used to check the current hybrid analytical–numerical approach. In Fig. 4, the results from the numerical approach are obtained under very fine discretization (space step = 0.05 cm and time step = 0.01 s) and strict convergence criteria (error between two consecutive interactions $< 10^{-6}$ mg/l). The same time step and convergence criteria are also used in numerically solving problem (9) for the hybrid analytical–numerical solution. As shown in Fig. 4, the results from the hybrid analytical–numerical solution are almost identical to the results from the numerical approach by Huang et al. [12].

Fig. 5 is a simplified example for purpose of illustration, as to how our solution can be used to simulate nonlinear iron oxide bioreduction with nonlinear sorption. In this example, iron oxide is reduced as an electron acceptor in a dissimilatory iron bioreduction process [15]. We assume that the carbon source and other nutrients are in excess such that the electron acceptor concentration is the only limiting factor on bioreduction rate. We also assume that this bioreduction process follows a Monod-type kinetic expression [18]:

$$\frac{\mathrm{d}C}{\mathrm{d}t} = \frac{(\mu_{\max}/Y)A}{K_s^A + A}X, \tag{18}$$

Here C is the concentration of bioreduction product Fe(II) (mmol/l); A is the concentration of iron oxide surface sites that are available for bioreduction (mmol/g), the $\mu_{\max}$ is the maximum growth rate (1/h), Y is yield (cell/mmol of iron), K_s^A is a half saturation coefficient for

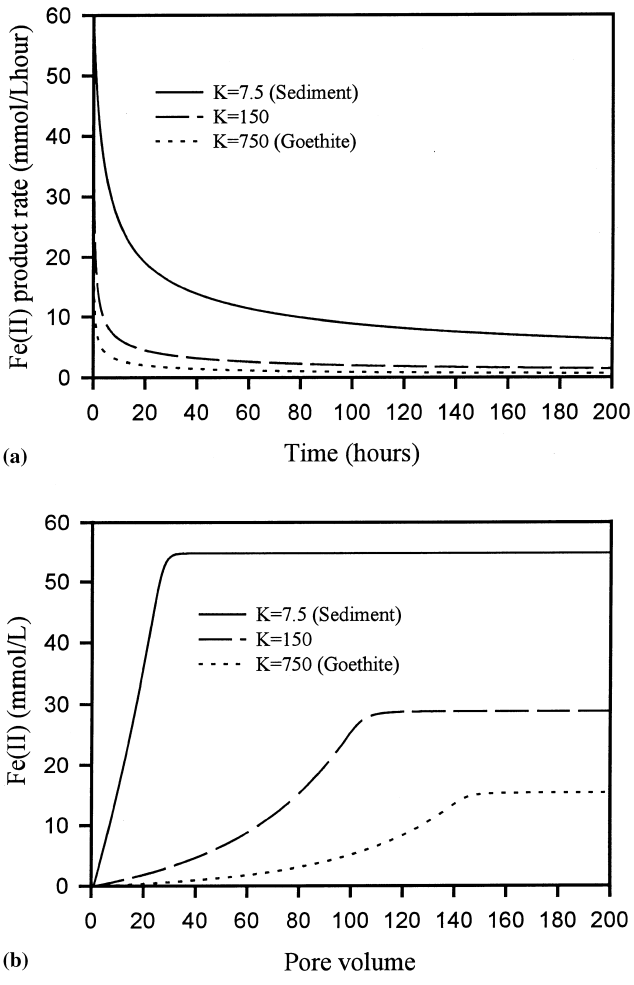

Fig. 5. Fe(II) concentration production during iron oxide bioreduction. Fig. 5(a) shows Fe(II) production rate with time in batch system. Fig. 5(b) shows Fe(II) breakthrough curves in a 20 cm column. Parameters used: dispersivity (α_L) = 0.1 cm; velocity (v) = 20 cm/h; bulk density (ρ_b) = 1.62 g/cm^3, porosity (ε) = 0.32; column length (L) = 20 cm; sorption isotherm $S = QKC/(1+KC)$; $Q = 1$ mmol/g; K (cm^3/mmol) (see plot insets); $I(C) = (\mu_{max}/Y)(Q-S)X/(K_s^A + Q - S)$; $\mu_{max}/Y = 1.21 \times 10^{-9}$ mmol/cell hour; $X = 10^8$ cell/ml; $K_s^A = 1$ mmol/g).

iron bioreduction (mmol/g), and X is cell density (number of cells/ml).

In this example, cell density is assumed to be constant because it has been observed that cell growth can often be ignored in iron bioreduction processes when initial cell concentration is about 10^8 cells/ml or higher [8,26]. Further, the iron bioreduction product, Fe(II), can have a strong nonlinear sorption on iron surface sites [23]. Here we assume that the sorption of Fe(II) on iron oxides surface sites follows a Langmuir isotherm model:

$$S = \frac{QKC}{1+KC}, \tag{19}$$

where K is an affinity coefficient (cm^3/mmol), Q is the maximum sorbed concentration (mmol/g), and S is the sorbed concentration (mmol/g). A site that is sorbed with Fe(II) is assumed to be unavailable for bioreduction.

We also assume that the iron oxide aggregate is large enough that the reduction process will not reduce the total number of iron surface sites and that only the sorption process will reduce the number of iron surface sites that are available for iron bioreduction. Under these assumptions, we have

$$A = Q - S. \tag{20}$$

Using Eq. (20) and (19) becomes,

$$\frac{dC}{dt} = \frac{(\mu_{max}/Y)(Q-S)}{K_s^A + (Q-S)}X. \tag{21}$$

Now considering Eq. (1a), we use Eq. (21) as $I(C)$ and Eq. (19) toward the estimation of a concentration dependent value of $R(C)$ to form our solute transport problem with nonlinear sorption and nonlinear reaction.

Fig. 5(a) shows iron bioreduction rate change with time in a batch system. This bioreduction rate can be derived from Eqs. (19) and (21)

$$\frac{dC}{dt} = \frac{Q\mu_{max}X/Y}{\sqrt{(2QKK_s^A\mu_{max}X/Y)t + (Q+K_s^A)^2}}. \tag{22}$$

As shown in Eq. (22) and Fig. 5(a), Fe(II) sorption on iron oxide surface sites has a strong effect on the bioreduction rate of iron oxide – i.e., on the rate at which Fe(II) increases. Eventually, bioreduction will stop when all the surface sites of iron oxide are occupied by the reduction product, Fe(II).

Strong sorption (high affinity coefficient, K) will not only reduce the aqueous concentration of Fe(II), but also reduce the overall bio-availability of iron oxides since a larger proportion of the Fe(II) will reside in the sorbed phase at any given time. Fig. 5(b) shows how these two processes lead to much lower breakthrough concentrations for the Goethite case, which has a higher Fe(II) affinity coefficient ($K = 750$) than the sediment case ($K = 7.5$). However, unlike batch systems, in which bioreduction process will eventually stop, the flow system will continuously remove Fe(II) produced during bioreduction. When this removal rate is the same as the production rate, then the system will reach a steady state, as shown in Fig. 5(b).

Fig. 6(a) and (b) show the effects of flow velocity on the bioreduction rate of iron oxides. As shown in Fig. 6(a), lower flow rates can have higher Fe(II) removal rate per unit volume of flow; however, and as shown by Fig. 6(b), the lower rates nevertheless have an overall increased time duration per unit mass of iron removal. As evident from Eq. (2) with sorption relation (19) and reaction Eq. (21), the removal rate per unit volume of flow will reach its maximum when the flow rate reaches its minimum, so long as some flow is maintained to avoid stopping bioreduction. However,

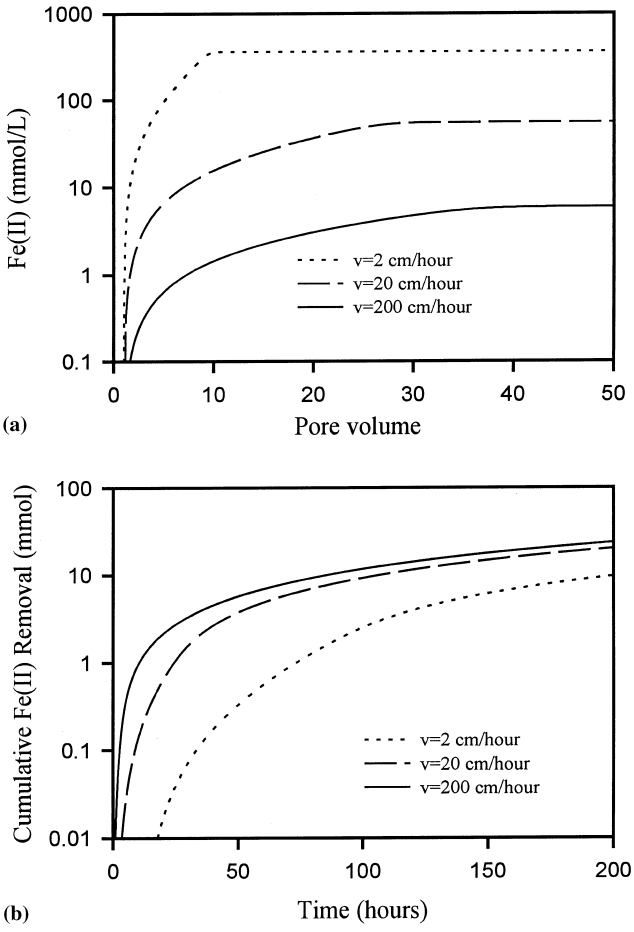

Fig. 6. Fe(II) breakthrough curves and cumulative Fe(II) mass removal from a column subject to iron oxide bioreduction under different flow velocities (see insets). Fig. 6(a) shows breakthrough curves and Fig. 6(b) shows total mass removal from the column ($K = 7.5\,\mathrm{cm}^3/\mathrm{mmol}$ and other parameters are the same as in Fig. 5).

the time duration per unit Fe(II) mass removal will reach its maximum at these low flow rates. In field or real experimental conditions, this trade-off between removal time and flow volume will be complicated by other factors, such as the type of iron oxide mineral surface (with associated effect on sorption characteristics), iron sorption on bacterial surfaces [23] and effects of variations in nutrients, carbon-sources, or other geophysical, geochemical, and biological factors. An optimal design of iron bioreduction system may need to consider all of these system conditions and their internal relations.

5. Conclusions

We have applied a generalized integral transform technique to solve solute transport problems under complex conditions of advection, dispersion, sorption, and decay. A general analytical solution has been developed for application toward linear cases of solute transport with space- and time-variable sorption, dispersion, flow, and decay. However, the applicability of the analytical solution to evaluate concentrations for any given practical problem depends strongly on the degree of difficulty in numerically evaluating the solution. Numerical evaluation of the solution can be greatly simplified for two broad classes of problems: (a) steady state flow and decay with arbitrary spatial functions of transport parameters; and (b) transitional flow, dispersion, and decay in homogeneous porous media. When either sorption, or decay, or both are nonlinear, solutions obtained by the GITT become hybrid analytical–numerical. In these cases, solution is still analytic with respect to space variables. However, the temporal part of the solution has to be solved numerically. For the examples explored in this paper, the solution converges fast when only nonlinear decay is considered (approximately 30 terms in the series solution); however, it becomes slow when there is nonlinear sorption (approximately 100 terms). Nevertheless, the accuracy of the solution derived by GITT can be controlled by controlling every numerical step with prescribed accuracy [4,5]. In this sense, solutions by the GITT for nonlinear problems have an important value as a means of obtaining benchmark solutions against which other potentially less computationally intensive methods might be compared.

Acknowledgements

This work is funded by the US Department of Energy, Natural and Accelerated Bioremediation Research Program (NABIR), Office of Biological and Environmental Research. Pacific Northwest National Laboratory is operated for the US Department of Energy by Battelle Memorial Institute.

Appendix A

This Appendix A serves to prove that matrix $\mathbf{A}(\mathbf{T})$ in Eq. (9a) is positive definite.

For any n by 1 vector $\mathbf{y}$, we have

$$\mathbf{y}^{\mathrm{T}}\mathbf{A}(\mathbf{T})\mathbf{y} = \int_0^L R(C,x)\mathbf{y}^{\mathrm{T}}\boldsymbol{\Phi}(x)\boldsymbol{\Phi}^{\mathrm{T}}(x)\mathbf{y}\,\mathrm{d}x = \int_0^L R(C,x)(\boldsymbol{\Phi}^{\mathrm{T}}(x)\mathbf{y})^2\,\mathrm{d}x \geqslant 0, \tag{A.1}$$

where $\boldsymbol{\Phi}(x)$ is n by 1 vector consisting of eigen functions

$$\boldsymbol{\Phi}(x) = \begin{bmatrix} \varphi_1(x)/N_1^{1/2} \\ \varphi_2(x)/N_2^{1/2} \\ \vdots \\ \varphi_n(x)/N_n^{1/2} \end{bmatrix}.$$

Eigen functions $\varphi_1(x), \varphi_2(x), \ldots, \varphi_n(x)$ are defined by Eq. (4a). Because all eigen functions are mutually orthogonal, the only condition that makes Eq. (A.1) equal zero is vector $\mathbf{y} = 0$. Therefore, $\mathbf{A}(\mathbf{T})$ is a positive definite matrix.

References

[1] Almeida AR, Cotta RM. Integral transform methodology for convection–diffusion problems in petroleum reservoir engineering. Int J Heat Mass Transfer 1995;38(18):3359–67.

[2] Bear J. Dynamics of fluids in porous media. New York: Elsevier, 1972.

[3] Brenner H. The diffusion model of longitudinal mixing in beds of finite length, numerical values. Chem Eng Sci 1962;17:229–43.

[4] Cotta RM. Hybrid numerical analytical approach to nonlinear diffusion problems. Numer Heat Transfer, Part-B-Fundamental 1990;17:217–26.

[5] Cotta RM. Integral transforms in computational heat and fluid flow. Boca Raton: CRC Press, 1993.

[6] Dagan G. Time-dependent macrodispersion for solute transport in anisotropic heterogeneous aquifer. Water Resour Res 1988;24(9):1491–500.

[7] Dankwerts PV. Continuous flow systems. Chem Eng Sci 1953;2:1–13.

[8] Fredrickson JK, Zachara JM, Kennedy DV, Dong H, Onstott TC, Hinman NW, Li SM. Biogenic iron mineralization accompanying the dissimilatory reduction of hydrous ferric oxide by a groundwater bacterium. Geochimica et Cosmochimica Acta 1998;62:3239–57.

[9] Freeze RA, Cherry JA. Groundwater. Englewood Cliffs, NJ: Prentice-Hall, 1979.

[10] Gelhar LW. Stochastic subsurface hydrology. Englewood Cliffs, NJ: Prentice-Hall, 1993.

[11] Goode DJ, Konikow LF. Modification of a method-of-characteristics solute-transport model to incorporate decay and equilibrium-controlled sorption or ion exchange. Water-Resources Investigation Report 89-4030, US Geological Survey, Reston, Virginia, 1989.

[12] Huang K, Mohanty PB, Leij FJ, van Genuchten MT. Solution of the nonlinear transport equation using modified Picard iteration. Adv Water Resour 1998;21:237–49.

[13] IMSL, IMSL Library, Math/Library, Houston, Texas, 1991.

[14] Liu C, Ball WP, Ellis JH. An analytical solution to one-dimensional solute advection–dispersion equation in multi-layer porous media. Transp Porous Media 1998;30:25–43.

[15] Lovley DR. Dissimilatory metal reduction. Ann Rev Microbiol 1993;47:263–90.

[16] Mikhailov MD, Ozisik MN. Unified analysis and solution of heat and mass diffusion. New York: Wiley, 1984.

[17] Moler C, van Loan C. Nineteen dubious ways to compute the exponential of a matrix. SIAM Review 1978;20(4):801–37.

[18] Monod J. The growth of bacterial cultures. Ann Rev Microbiol 1949;3:371–93.

[19] Ozisik MN. Heat Conduction. New York: Wiley, 1993.

[20] Parker JC, van Genuchten MT. Flux-averaged and volume-averaged concentrations in continuum approaches to solute transport. Water Resour Res 1984;20:866–72.

[21] Press WH, Teukolsky SA, Vetterling WT, Flannery BP. Numerical recipes. Cambridge, MA: Cambridge University Press, 1992.

[22] Rugh WJ. Linear system theory. Englewood Cliffs, NJ: Prentice-Hall; Simon & Schuster/A Viacom Company, 1996.

[23] Urrutia MN, Roden EE, Fredrickson JK, Zachara JM. Microbial and surface chemistry controls on reduction of synthetic Fe (III) oxide minerals by the dissimilatory iron-reducing bacterium. Geomicrobiology 1998;15:269–91.

[24] van Genuchten MT, Alves WJ. Analytical solutions of the one-dimensional convective–dispersive solute transport equation. USDA Tech Bull 1982;1661.

[25] van Genuchten MT, Parker JC. Boundary conditions for displacement experiments through short laboratory soil. Soil Sci Soc Am J 1984;48:703–8.

[26] Zachara JM, Fredrickson JK, Li, S-M., Kennedy DW, Smith SC. Bacterial reduction of crystalline Fe(III) oxides in single phase suspensions and subsurface materials. Am Mineralog 1998;83:1426–43.